World Academy of Science, Engineering and Technology
International Journal of Aerospace and Mechanical Engineering
Vol:11, No:1, 2017

Hybrid Rocket Motor Performance Parameters: Theoretical and Experimental Evaluation

A. El-S. Makled, M. K. Al-Tamimi

***Abstract*—**A mathematical model to predict the performance parameters (thrusts, chamber pressures, fuel mass flow rates, mixture ratios, and regression rates during firing time) of hybrid rocket motor (HRM) is evaluated. The internal ballistic (IB) hybrid combustion model assumes that the solid fuel surface regression rate is controlled only by heat transfer (convective and radiative) from flame zone to solid fuel burning surface. A laboratory HRM is designed, manufactured, and tested for low thrust profile space missions (10-15 N) and for validating the mathematical model (computer program). The polymer material and gaseous oxidizer which are selected for this experimental work are polymethyle-methacrylate (PMMA) and polyethylene (PE) as solid fuel grain and gaseous oxygen (GO_2) as oxidizer. The variation of various operational parameters with time is determined systematically and experimentally in firing of up to 20 seconds, and an average combustion efficiency of 95% of theory is achieved, which was the goal of these experiments. The comparison between recording fire data and predicting analytical parameters shows good agreement with the error that does not exceed 4.5% during all firing time. The current mathematical (computer) code can be used as a powerful tool for HRM analytical design parameters.

***Keywords*—**Hybrid combustion, internal ballistics, hybrid rocket motor, performance parameters.

I. Introduction

HIGH demand on safe and low cost commercial space applications increases the interest on hybrid propulsion systems (HPS). In response, a number of governmental laboratories, large industrial companies, academic research institutions, and small foundations implement hybrid rocket research and development efforts that led during the past decade to significant state-of-the-art advancements in HPS.

The HRM is a promising trademark of space propulsion applications [1], [2]. Many benefits are demonstrated and realized during the last years as green combustion, acceptable performance, controllable, high reliability, re-ignition capability, low cost, high safety, and available technology. HRM as a state of the art, needs continuous justification of some drawbacks from variations of performance parameters during firing (regression rate, chamber pressure, thrust and fuel mass flow rate), low regression rate, and low combustion efficiency [3], [4]. A simplified schematic-diagram of classical HRM and other versions (pan-cake, inverse and complex) are given in Fig. 1. Generally, In HRM, one of the propellants is solid fuel or compound solid fuel, and the other one is liquid or gas oxidizer. The different states and separation of fuel and oxidizer are the main reason of being better than either solid or liquid propulsions.

The work started with the normal research stages as design, manufacture, and firing of the laboratory small thrust HRM. Preliminary design produced and parameters verification for real design can be used in development of space propulsion applications as launch correction, orbit transfer, orbit correction, and de-orbiting missions.

The objective is to predict the variation of operating parameters during firing as chamber pressure, thrust, fuel mass flow rate, mixture ratio, and regression rate. It is discovered that the most important parameters are convective and radiative heat transfer produced by the combustion process, which strongly affects the vital regression rate parameter.

The mathematical (computer) model evaluation is performed by comparison between experimental and numerical data. This computer code can be used also to characterize a newly designed HRM performance and to simulate the effect of various design parameters.

The principal requirement for the design of HRM is the availability of means to predict the IB parameters under all operating conditions. The IB of HRM differs markedly from those in liquid and solid propulsion systems. The hybrid combustion process is controlled by flame zone heat transfer inside boundary layer above fuel regression surface. Understanding of hybrid combustion IB is dependent upon the assessment of the correlation between the boundary layer characteristics and fuel grain geometry during firing time.

The lack of HRM development resulted in a relatively immature technical knowledge of IB hybrid combustion compared to that of solid and liquid combustion phenomena. The hybrid combustion process relies on a host of different parameters, which has made it difficult to develop a global model. Low combustion efficiency due to incomplete combustion is stated in many references [3]-[5].

Ah. El-S. Makled was with Military Technical College, Cairo, Egypt. He is now with the Space Technology Center, Cairo, Egypt (phone: 2 010 03784889, e-mail: Ahmak2007@yahoo.com).

M. K. Al-Tamimi is PhD student at the Military Technical College, Cairo, Egypt (e-mail: m_altimimi@hotmail.com).

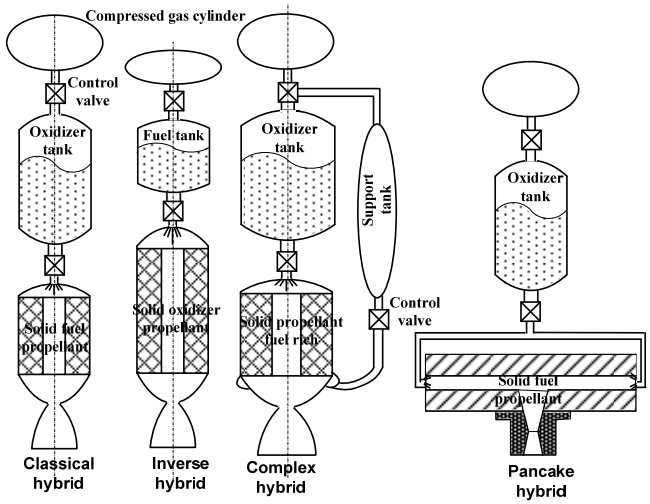

Fig. 1 General schemes of HPS types

II. Theoretical Work

The mathematical model for calculating the behavior of IB parameters is dependent on an understanding of combustion, heat transfer, and flow phenomena inside the active channel port of solid fuel grain.

A. Basic Assumptions

Theoretical equations used in mathematical model are derived from IB of solid fuel flat-plate combustion, using slab burner with PMMA as solid fuel and GO_2 as oxidizer. The slab burner is considered as pure HRM with fairly simple grain configurations (without any sharp corners and energetic material within the fuel grain), and the following major assumptions are considered as [6]-[8]:

1. Solid fuel flat plate with turbulent combustion boundary layer,
2. Regression rate of grain is controlled by heat transfer from a diffusion thin flame zone,
3. Oxidizer enters active port as a uniform gaseous stream,
4. No heat is transferred into subsurface region of solid grain,
5. Pressure and oxidizer mass flow rate are constant along the plate and varies only with time,
6. Lewis number (the ratio of thermal diffusivity k_f to the self-diffusion coefficient) $L_e = {k_f}/{C_p \rho}$ and Prandtl number (the kinematics viscosity to thermal diffusivity) $P_r = {C_p \mu}/{k_f}$ are both equal 1, where C_p is the specific heat at constant pressure, and μ is the dynamic viscosity.

B. Hybrid Combustion Mechanism

The variations of combustion chamber pressure Pc, thrust F, regression rate $\dot{m}_{fu}$, generated fuel mass flow rate $\dot{r}_{fu}$, mixture ratio O/F, and fuel grain port diameter d_{po} with firing time are required to describe the IB combustion model. For better understanding of the behavior of these parameters, it is useful to describe the combustion mechanism. Hybrid combustion occurs in a thin flame zone within the turbulent boundary layer over solid fuel burning surface as shown schematically in Fig. 2. In the presented case of study, where solid fuel grain surface is internally burned, fuel is decomposed and evaporated (gasified) at the solid surface by convective and radiative heat transfer from flame zone. It diffuses inward toward the centerline of the fuel grain active channel (combustion chamber). Simultaneously, gaseous oxidizer diffuses outward from the center-line through the turbulent boundary layer to the burning surface. At a point where the mixture ratio concentration corresponds to stoichiometric O/F, complete combustion occurs in a layer whose thickness is of the order of 10% of the boundary layer thickness, and this zone is called the flame zone [9]. The rate of combustion is governed by the rate at which heat is transferred from the flame zone to the solid fuel surface rather than by chemical kinetics of the reaction.

C. Hybrid Combustion Model

The IB combustion modeling deals primarily with the transport of heat by convection and radiation from the diffusion flame zone (located in the turbulent boundary layer) to the solid surface as shown in Fig. 2. The equation of energy conservation can be written as:

(flame zone to fuel surface) $\dot{Q}_{Convection,\ in} + \dot{Q}_{Radiation,\ in} =$ $\dot{Q}_{Conduction,\ out}$ (fuel surface to depth of solid fuel grain) + $\dot{Q}_{Radiation,\ out}$ $\left(= k_f \frac{\partial T}{\partial y}\right.$ solid fuel surface to surroundin g) + $\dot{Q}_{Phase\ change,\ out}$ $\left(= \rho_{fu} \dot{r}_{fu} h_{veff}\right.$ at solid fuel surface)

The dependence of solid fuel surface regression rate on the convective heat transfer and the radiative heat transfer may be given by [8]:

$$\rho_V \dot{r}_{fu} = \pi \rho_{fu} (1-K) \dot{r}_{fu} = \left(\frac{\dot{Q}_c}{h_{veff}}\right)\left[\left(\frac{\dot{Q}_r}{\dot{Q}_c}\right) + e^{-\frac{\dot{Q}_r}{\dot{Q}_c}}\right] \quad (1)$$

$$\dot{Q}_c = 0.036 \left(\frac{\dot{m}_g}{A_{po}}\right)^{0.8} \left(\frac{x}{\mu}\right)^{-0.2} h_{veff}\, \beta^{0.23} \quad (2)$$

$$\dot{Q}_r = \alpha \varepsilon T_r^4 \left(1 - e^{-\alpha N}\right) \quad (3)$$

$$G_{tot} = \left(\frac{\dot{m}_g}{A_{po}}\right) \quad (4)$$

where, ρ_v : Bulk density of volatile component of fuel grain, ρ_{fu} : Density of fuel grain, k: mass fraction of non-volatile surface material, X: Distance along fuel grain port, μ: Viscosity of combustion gases, β: Mass transfer number, h_{veff}: effective heat of gasification (vaporization) of solid phase, α: empirical radiation coefficient, ε: Emissivity of the fuel grain surface, T_r : effective radiation temperature, N: Radiation parameter in gas-phase emissivity. $\dot{m}_g$: total gas flow rate, A_{po}: effective port area, h: convective heat transfer coefficient from gas, ΔT: temperature difference between the flame zone and the fuel

surface, $\frac{\partial T}{\partial y}$: temperature gradient (in = flame to surface, out = surface to surroundings).

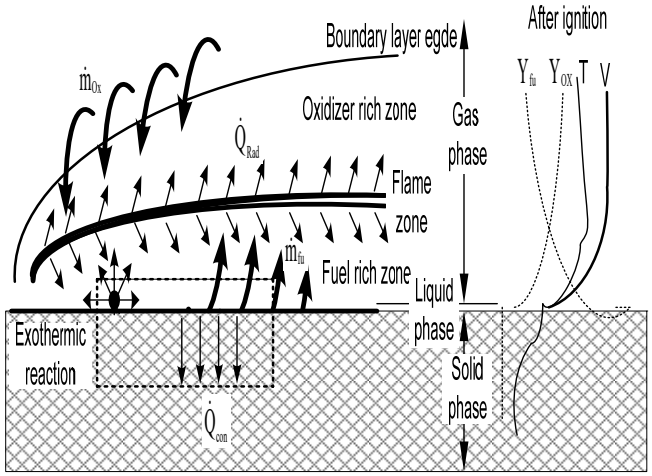

Fig. 2 Combustion zones and mechanisms of heat transfer for hybrid combustion

The regression rate described in (1) represents the coupling that occurs between convection and radiation heat transfer from a thin diffusion flame zone to the solid surface given by (2) and (3). It depends upon the total local mass flux G_{tot} given by (4) and the combustion chamber pressure P_c.

The effective radiation temperature T_r is estimated as 2/3 of the stochiometric temperature, which can be calculated from thermochemical code analysis [10]. The surface fuel grain temperature is assumed to be 600 to 800 K.

The local O/F at the flame zone is known to be fuel rich, and is estimated as ¾ stochiometric O/F [10]. It is considered independent of axial fuel grain length. The effective wall emissivity= 0.90 as estimated by Woolridge and Muzzy [7].

In large combustion chambers or in combustion gases containing large number of solid particles, an important part of the energy absorbed by the fuel surface may be radiant heat.

D. Hybrid Combustion Model

In a non-metallized fuel grain polymer as PMMA and PE, heat transfer by convection is much larger than that transferred by gas phase radiation [7]. As a result, the basic characteristics of the fuel regression may be explored via an analysis of convective heat transfer in the boundary layer. Neglecting the radiation heat transfer is regarded as a reasonable approximation and this would considerably simplify the treatment.

Neglecting radiation and conduction terms in (1), the energy transferred to the fuel surface by convection will be consumed in gasification of the solid phase.

$$\dot{Q}_s = \rho_{fu}\,\dot{r}_{fu}\,h_{veff} \tag{5}$$

This equation is used by Marxman [6] to obtain a semi-empirical formula of the regression rate given by:

$$\dot{r}_{fu} = 0.036\,\frac{G_{tot}^{0.8}}{\rho_{fu}}\left(\frac{\mu}{x}\right)^{0.2} B^{0.23} \tag{6}$$

It may be seen that hybrid fuel regression rate for a non-radiative system is strongly dependent on total mass flux and rather weakly on axial location x and fuel blowing characteristic B. One may also note that the regression rate is not explicitly dependent on chamber pressure in this treatment. Some fuels do not depend on chamber pressure while others exhibit a strong dependence. In particular, metallized hybrid fuel system exhibits a pronounced pressure dependency [7].

E. Total Mass Flow Calculation

The total gas flow can be described at any point of the gaseous stream of the combustion products, f(x), which is composed of the rate of head-end oxidizer flow plus the gas evolved from the surface minus the oxidizer consumed in the combustion. This can be described by [7]:

$$\dot{m}_g = \dot{m}_{ox} + (1 \quad k_1 \quad k_1\zeta_1)\int_0^x \rho_v\,\dot{r}_{fu}\,P\,dx \tag{7}$$

where k_1: mass fraction constant, volatile with particulate combustion products, P: internal perimeter of fuel grain. This equation assumes that a completely vaporizing grain produces particulate combustion products. The factor ξ1 accounts for the mass of oxidizer consumed in producing these particles.

F. Effective Fuel Grain Port Calculation

The basic geometry of HRM, including the active channel port is given in Fig. 3. The regression rate must be coupled through IB analysis to produce equations describing the instantaneous port geometry of the grain. The effective port area Apo is calculated by the actual port area subtracted from it the area occupied by the boundary layer displacement thickness [9].

$$\begin{aligned} A_{PO} &= \frac{\pi}{4}\left(d_{PO} - 2\delta^*\right)^2 \\ 2\delta^* &= 0.21 d_{PO}\left(\frac{x}{x_A}\right)^{0.8} \ldots\ldots\ldots x \le x_A \\ 2\delta^* &= 0.21 d_{PO} \ldots\ldots\ldots x \ge x_A \end{aligned} \tag{8}$$

where δ^* is the boundary layer displacement thickness and x_A corresponds to the merge point of the boundary layers.

As the fuel port area increases with time, the regression rate tends to decrease. To simulate this, the program divides the burning duration into finite time steps. After regression rate values are determined over each distance increment, each value is multiplied by the time interval to calculate the corresponding change in port diameters at each position:

$$d_{po,(New)} = d_{po(old)} + 2\dot{r}_{fu}(x)\Delta t \tag{9}$$

Thus, new values of the port area are determined which are used to calculate new values of regression rate at this time.

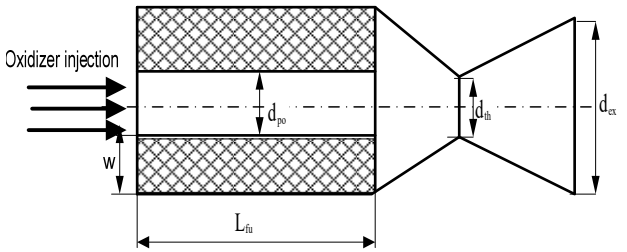

Fig. 3 Basic geometry of HRM

G. Nozzle Throat Diameter Calculation

During HRM operation, the nozzle dimensions may change after a certain delay time of firing t_{delay} due to thermal expansion and nozzle erosion depending on the nozzle material. In the present analysis, the nozzle throat diameter d_{th} versus time is defined by:

$$d_{th} = d_{th,o} + 2E_n\left(t_b - t_{delay}\right) \tag{10}$$

where E_n is the radial erosion rate of nozzle throat material, and t_{delay} is the delay time of erosion.

H. Tail-off Calculation

During tail-off, the oxidizer mass flow rate stops suddenly, the remainder of combustion gases is simply exhausted via the nozzle part. In the other words, this regime is characterized by zero regression surfaces and zero oxidizer mass flow rate. The rate at which the chamber pressure drops with time is relatively high; the pressure is computed from [10]:

$$P_c = P_D \exp\left[\Gamma^2 c^* \frac{\pi}{4} d_{th}^2 \left(t - t_D\right) / V_{cf}\right] \tag{11}$$

where c* is the characteristic velocity, t is the instantaneous time of calculation, P_D is the pressure at the end of steady state operation regime or the final pressure just before break-up (for t = tD), and V_{cf} is the final chamber volume.

III. Computation Solving Technique

The solution strategy that is adapted to determine the IB and performance parameters history can be described by Fig. 4 (a).

On performing these calculation loops, all the performance parameters could be evaluated. A flow chart of the implemented program is shown in Fig. 4 (b).

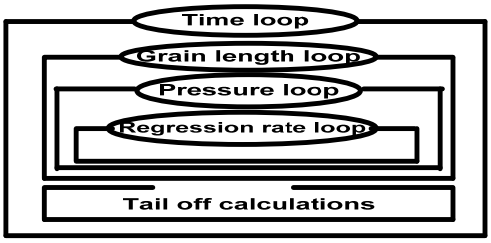

(a) Schematic loops solving technique

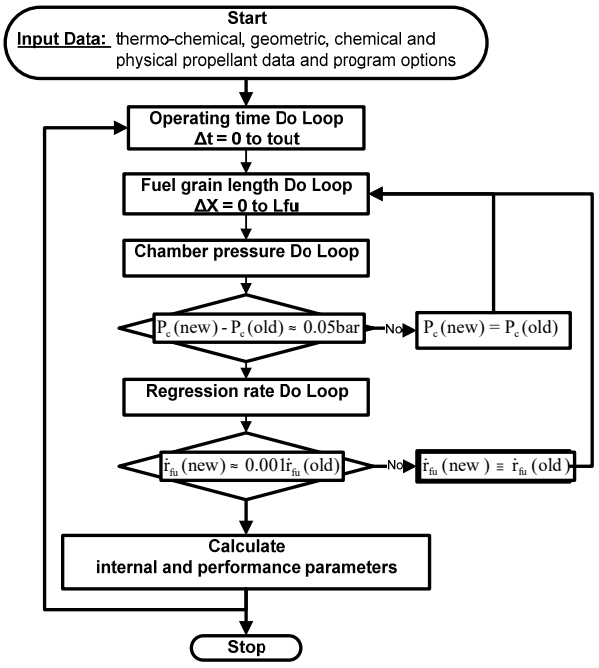

(b) Flow chart program

Fig. 4 Schematic loops and flow chart program of computation technique (computation software program)

A. Time Loop

A time step ≈0.1s is chosen as a base for the calculation. For each time step, the following parameters are determined by the completion of all internal loops (d_{po}, P_c, $\dot{m}_{ox}$, c*, thrust coefficient C_f, d_{th}, $\dot{m}_{tot}$, specific impulse I_{sp}, F, O/F, $\dot{m}_{fu}$, and total mass loss of fuel grain m_{fu}).

The firing time (counter timer) is then compared with burnout and quit time. If one of them is reached, the run is terminated and displays an acknowledgement message.

A check is made at each time step over the web thickness, to make sure that a new enlarged port does not go beyond the allowable web thickness. If web burnout occurs, the program stops and displays an acknowledgement message about this case. Otherwise, the program returns and calculates new values of regression rate for this new time interval corresponding to the enlarged port area. The time step loop continues in this manner until the quit time (estimated end of firing) is reached.

B. Pressure Loop

An initial pressure is assumed for the program initiation. After the internal loops within the pressure loop is completed, a new value for the pressure will be generated. The process of calculation will be repeated for the new pressure until the difference between two successive values falls within the permitted error.

C. Grain Length Loop

The grain length is divided into a number of distance increments. At each increment, the regression rate can be calculated as will be explained in the following loop. Consequently, the local fuel consumption is readily available

for use with the next distance increment. Having completed this loop, it returns the total mass flow rate of fuel. At that point, dividing the oxidizer flow rate by the fuel flow rate provides the mixture ratio. This is the checking parameter that will be used to correct the pressure allocated in the pressure loop. The approach is explained as follows; in a preparatory stage, thermochemical calculations are performed separately using a standard code [10] to establish a matrix array for the c^*_{th}= fun (O/F, Pc) in the domain inscribed between ($(O/F)_{min}$ - $(O/F)_{max}$, $(Pc)_{min}$- $(Pc)_{max}$)). This matrix is input to the present program. For the values of O/F and P_c being now known and with the help of linear interpolation, the value of $c^*_{th}$is deduced from the matrix array.

A new value for the pressure is calculated from:

$$P_{c,new} = \frac{\dot{m}_{tot} c^*_{th}}{A_{th}} \quad (12)$$

In this equation, the total mass flow of gases is the sum of the mass flow rate of oxidizer and the calculated mass flow rate of fuel. The nozzle critical diameter is corrected for erosion in accordance with the proposed model depending on t_{delay}. If needed, the new pressure value is forwarded to the pressure loop for a new iteration.

For each distance increment Δx, the following parameters are determined by d_{po}, A_{po}, $\dot{r}_{fu}$, G_{tot}, O/F. At the end, the program displays the maximum burning time that is reached, average values of fuel mass flow rate $\overline{\dot{m}}_{fu}$, and average regression rate $\overline{\dot{r}}_{fu}$.

D. Regression Rate Loop

One of the most difficult hybrid parameters to evaluate is the regression rate of the solid fuel grain. This parameter must be known as a function of grain length increment and firing time step in order to determine the accurate performance and combustion characteristics during firing time.

The regression rate is first calculated at the head end of the fuel grain based upon a value of the oxidizer mass flow entrance as a total mass flow rate and the initial port area. This regression rate is assumed constant over the small distance increment, adding mass to the stream flow. The calculated regression rate for the next finite increment is based upon accumulated mass flow through the port. Thus, it can be calculated down the length of the grain.

Once the exact regression rate is known over each distance increment ΔX, the value of fuel flow rate, the total mass flow rate through fuel port, O/F and the throat area are determined.

IV. Performance Calculation

Once the regression rate is known for each distance increment down the length of the fuel grain, the corresponding fuel emission values are summed up to get the total mass flow rate of fuel. The resulting O/F should lie within the limits specified in the input data, otherwise modification of data is needed. Using total mass flow rate and the input data (c*, combustion efficiency ηc and dth), the chamber pressure is calculated as:

$$P_c = \frac{c^* \dot{m}_{tot}}{\eta_c A_{th}} \quad (13)$$

The assumed and calculated values of chamber pressure are compared. If difference is not within a specified tolerance, the assumed value is replaced by the calculated pressure and used to determine a new fuel mass flow rate, O/F ratio, total mass flow rate, and pressure. This iteration process is continued until the difference between two successive values of chamber pressure falls within 0.05 bar.

As the fuel regression rate changes and consequently the total mass flow rate, the chamber pressure varies during burning time.

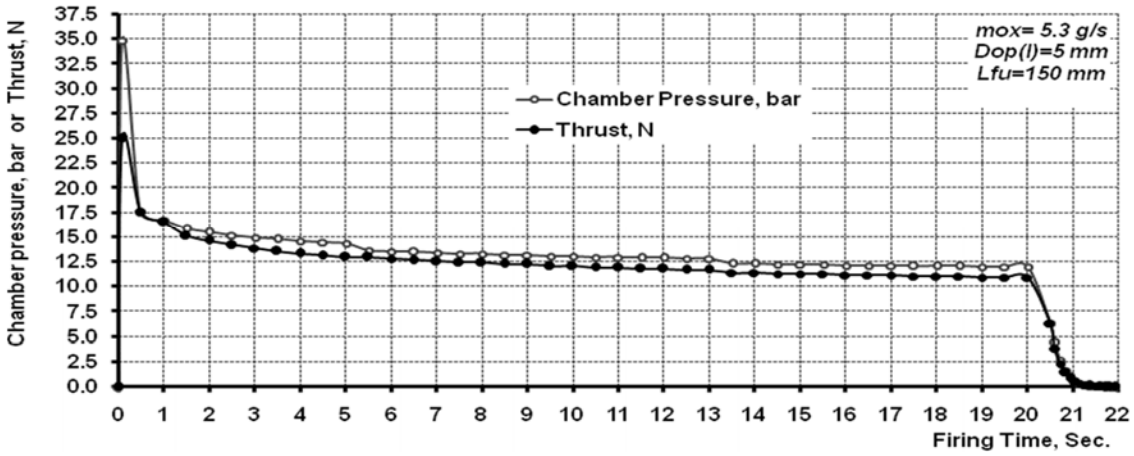

Fig. 5 Calculated chamber pressure and thrust with firing time

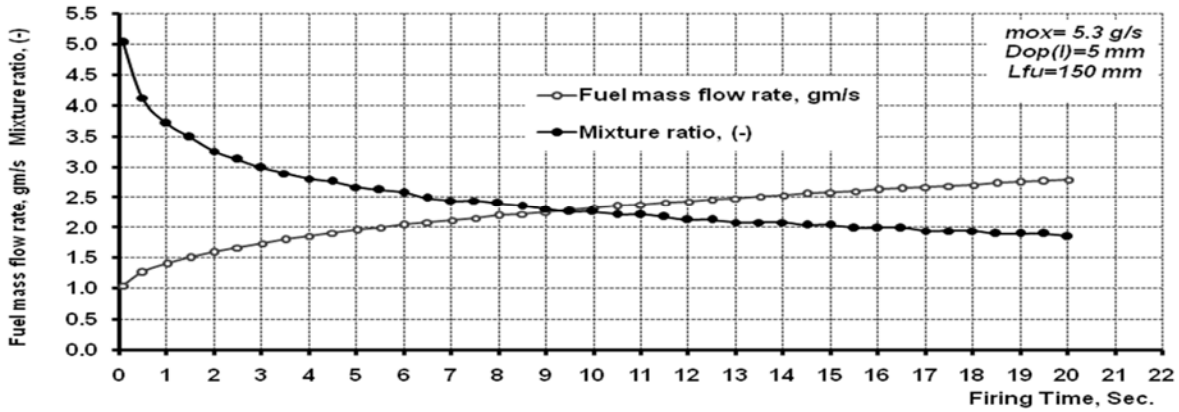

Fig. 6 Calculated fuel mass flow rate and mixture ratio with firing time

Once the regression rate is determined, the calculation of fuel flow rate and mixture ratio is performed as:

$$\dot{m}_{fu,new} = \dot{m}_{fu,old} + \int_{x=0}^{x=L_{fu}} \rho_{fu}\, \dot{r}_{fu}\, \pi\, d_{po}(x,t)dx \quad (14)$$

and the mixture ratio O/F:

$$O/F = \frac{\dot{m}_{ox}}{\dot{m}_{fu}} \quad (15)$$

Having correctly determined the chamber pressure and regression rate, the other performance parameters can be easily determined as shown in Figs. 5 and 6.

V. Experimental Work

To validate the computer code, a laboratory HRM is designed, manufactured, and tested. Over 30 firing tests using PMMA and PE as solid fuel and GO_2 as oxidizer and about five tests using PMMA are performed to investigate the suitable ignition method and adjust the operating parameters.

The laboratory test facility comprises two parts; test stand zone (test bed, camera, feeding system and safety area) and control room (computer system, recording data acquisition and calibration instrumentations for measuring tools). To minimize the risk of damage during firing, cold testing (hydrostatic test) is accomplished on the HRM and oxidizer feeding line by applying a 25-bar static pressure for 10 minutes checking that no leakage or failure occurred at all fitting connectors. Silicon materials create a static seal and they are employed to ensure a static force seal for the HRM, which are good for GO_2 and fuel polymer environments. Fig. 7 describes the HRM, required items for GO_2 feeding system, and measuring devices locations. For achieving a successful firing, it is necessary to make several attempts to adjust the operational motor parameters and ignition system. Hot testing is accomplished using a test bed (0.5ton max. thrust) as shown in Fig. 8.

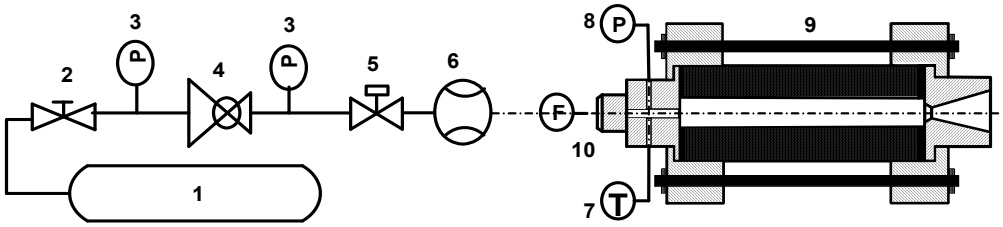

Fig. 7 Feeding system 1-Oxidizer tank, 2-Needle valve, 3- Pressure gage, 4- Pressure regulator, 5- On-off valve, 6-Rotameter, 7-K Type Thermocouple, 8-Pressure transducer, 9- HRM, 10- Thrust transducer

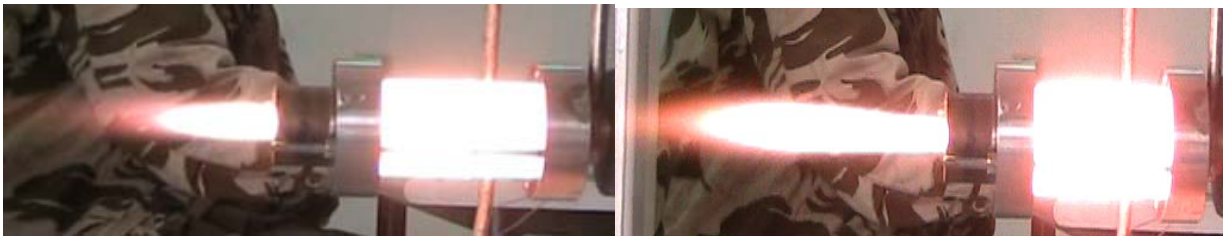

Demonstration tests

Real firing tests

Fig. 8 PE+GO_2 Firing Sample Function Tests

A. Pyrotechnic Ignition Method

The ignition is established by using squibs (bridge resistance 3 Ω, minimum operating current 1 A). The squib is introduced via nozzle critical section to tough fuel grain surfaces. For more reliability, a 0.25 g of black powder is provided around the sensitive element to act as flame amplifier with ignition impulse 20 bar as shown in Fig. 9 (a).

The ignition procedure by pyrotechnic charge in hybrid system is described in Fig. 9 (b). The procedure is summarized as,

- Adjust feed system.
- Open the GO_2 line by solenoid valve command (ON).
- After approximately 0.25 s, the 30-Volt DC 5A current pass through squib to produce a flame of heated gases. The initial burning surface is melted and evaporated. Vaporized gases react with the oxidizer media to start combustion.

This method showed a small ignition delay time about 0.4 s.

With a too high mass flux of oxidizer, several ignition failures occurred. The reliability increases to maximum with low oxidizer mass flux. Fig. 9 (c) describes a sample of obtained pressure and temperature with time using pyrotechnic charge.

B. Laboratory Hybrid Rocket Motor (HRM)

Fig. 7 shows the main parts of the tested HRM. The HRM test is designed for quick and simple hook up to gas supply system. Teflon tube with length about 1 m is used for gas feeding to provide safety against hazardous fire at the GO_2 line supply and to offer a high degree of freedom of the motor on the test bed to accurately measure the axial thrust. Only two sides of fuel grain are protected by 2 mm Teflon gasket from any thermal effects. The cheapest functional nozzle material like red copper is selected. Table I gives the main design parameters of HRM.

(a) Squib igniter

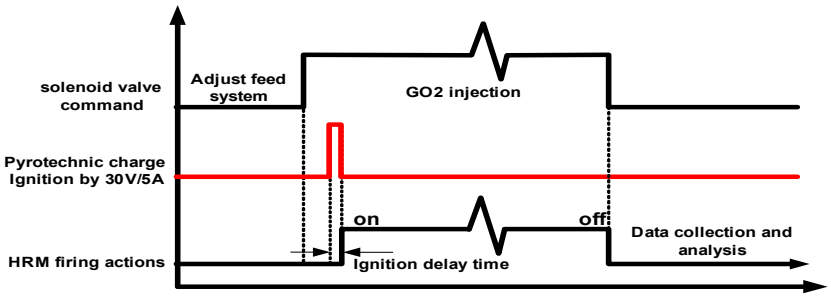

(b) Ignition procedure

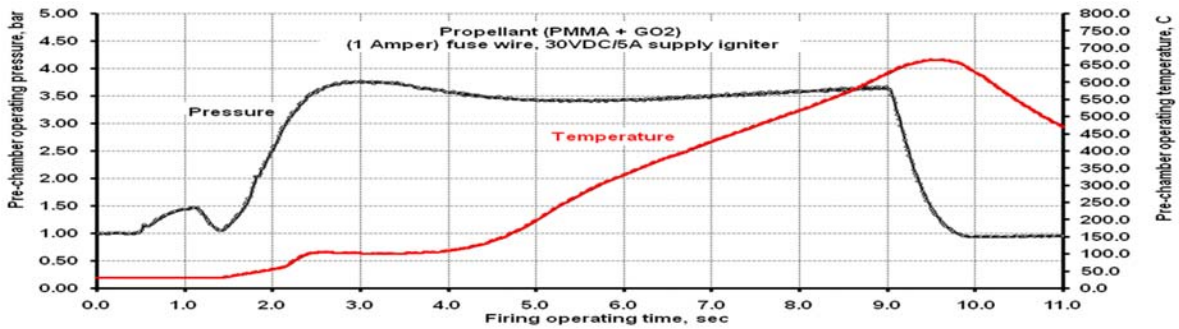

(c) Pre-chamber pressure and temperature with firing time Fuel

Fig. 9 Activities of pyrotechnic igniter

TABLE I
SMALL-SCALE HYBRID MOTOR CHARACTERISTICS

Parameter	Value
Maximum thrust value (N)	25
Oxidizer flow rate (g/s)	2.5 to 10
Initial port diameter (mm)	5 to 30
Fuel grain length (mm)	50 to 160
Mean regression rate (mm/s)	0.05 to 0.85
Injection pressure (bar)	5 to 20
Maximum chamber pressure (bar)	20
Firing time (s)	5 to 20
Nozzle throat diameter (mm)	3.0
Combustion efficiency	90 to 95%

C. Oxidizer Feeding System

Fig. 7 describes the HRM gas supply system components; industrial GO_2 bottles used up to minimum pressure 30 bar with pressure regulator is used to control GO_2 mass flow. A rotameter with maximum scale 15 g/s, located just upstream of HRM is used to measure the precise GO_2 mass flow rate. Solenoid valve (220V, 3A when loaded) is introduced in the supply line to allow on-off control from the control room. The solenoid valve and ignition spark order are engaged from relay switch connected to the data acquisition board, to make sure that the combustion chamber is full of GO_2 before spark ignition. The system employs stainless steel tubing of 6mm outer diameter for high pressure line and tubing from hard rubber material for low-pressure line with the same diameter. Swagelok fittings are used in most cases, whereas other fittings are used with sensors. The HRM system is operated from control room, and the duration of GO_2 supply phase and ignition time can be adjusted from the control room.

D. Data Acquisition System

The system allows performing measurements on feed line, oxygen tank, combustion chamber pressures, and oxygen flow rates. Besides, two channels are used for thrust measurements during the test run. Other variables are measured before and after a test run: ambient temperature, nozzle throat, and exit diameters (dial counter vernier caliber, accuracy 0.01 mm). Masses of the fuel grain are measured by using a digital mass scale of accuracy 0.01 gram.

The system includes an Ultraviolet recorder (Shandon southern instruments limited, England, type F10-352), analogue (magnetic) tape recorder (Sedeme, model 101), AD converter (Sedeme at France, max. frequency 10 kHz), and digital tape recorder. The Ultraviolet recordings only serve for a quick first-look analysis, and the signals recorded by the digital tape recorder are directly used as an input for computerized data reduction. The analogue signals from the analogue tape recorder are used as back up and for replay in some cases of unexpected events. The system is adjusted to read 1000 points per second, and five channels are used during test (two channels for thrust and three channels for pressure). For the analysis of data, a special computer code is developed to comply with hybrid system.

VI. EVALUATION OF THE MODEL

In order to check the validity of the developed mathematical model, measurements are made by real firing, and the experimental data are compared with the model predictions.

Table II presents a sample of the predicted and measured results. The validity of the model is proven by the good agreement as it is evident from the comparison. The maximum error is generally less than 4.5%. An exception is seen regarding the thrust, which may be attributed to the high amplitude oscillations encountered during the measurement.

TABLE II
COMPARISON OF COMPUTED AND MEASURED RESULTS

Parameter	Analytical	Experimental	Error %
Average chamber pressure (bar)	13.22	13.46	1.8
Thrust (N)	10.31	10.94	6.1
Mixture ratio (-)	2.53	2.48 to 2.55	1.4
Regression rate (mm/s)	0.36	0.33 – 0.36	4.3
Fuel mass flow rate (g/s)	2.15	2.14	0.35

In Fig. 10, chamber pressure and thrust time obtained from computer program are compared with the test results. It can be seen that the theoretical calculated values at about the first two seconds are somewhat greater than the values from test. However, the error is gradually decreased to about 1.5% at the end of firing time. This can be explained by the fuel regression in the ignition period which is neglected and by the interdependence of a great number of the assumed input variables, being too difficult to be accurately estimated.

Fig. 10 displays typical combustion instability that reaches 0.8 bar, and less than 0.5 s is required for pressure to reach its operating regime after ignition.

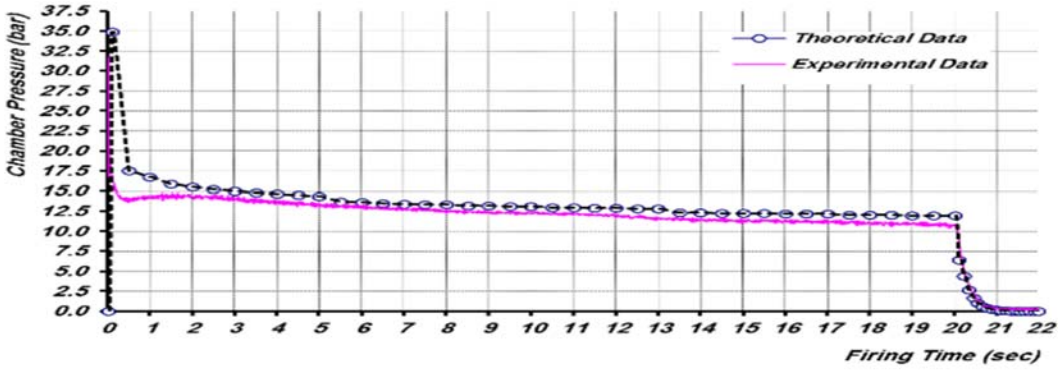

(a) Experimental and theoretical chamber pressure

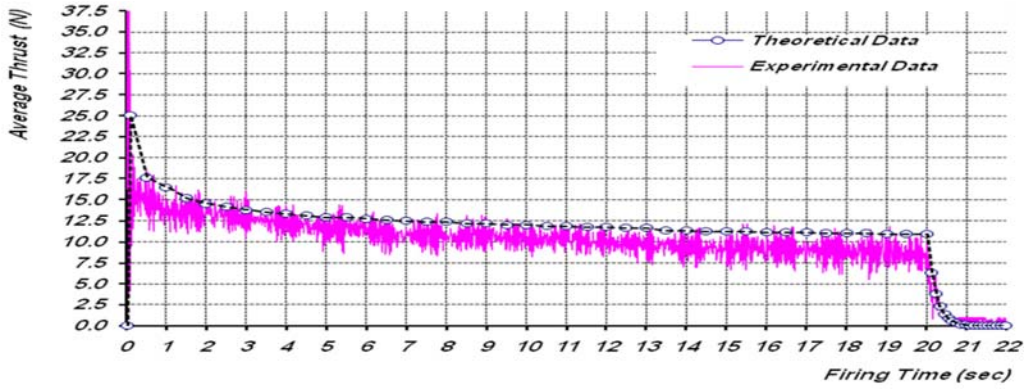

(b) Experimental and theoretical thrust

Fig. 10 Comparison between theoretical and experimental performance data (at $\dot{m}_{ox}$= 5.5 g/s, L_{fu}= 150 mm, $D_{po(i)}$= 5 mm)

The large pressure drop during the first half of the firing time may be attributed to the relatively small initial port diameter, and therefore higher oxygen mass flux, which revealed to a rapid change in active channel port dimensions. The pressure is decreased by approximately 10 to 12.5% of the main value during the firing duration. It may be justified to neglect the ignition time, being too small compared to the firing time, whereas the tail off period, lasting about 0.9-0.8 s should be considered when calculating the performance of the HRM.

VII. Conclusion

A computer code based on a simplified theoretical model is developed to predict the parameters of hybrid rocket motors employing tubular fuel grain configurations. The flexibility of the program, which can be run on a personal computer, makes it a valuable preliminary design tool for hybrid rocket motors. As compared with the test results, the prediction error does not exceed 4.5% during the first 5 s and drops to 2% at the end of firing. Obviously, the selection of fuel grain characteristics has a significant impact on the hybrid motor performance, which is largely a function of the combustion phenomena. The program can be used to evaluate quantitatively the effect of changes in various design parameters, e.g. to examine the changing effect of oxidizer mass flow, fuel port diameter, fuel grain length and fuel grain types on the hybrid rocket motor performance.

References

[1] Migireanu F. "Small Launcher Enabled by Hybrid Rocket Motor Technology" 17th Int. Conference on Applied Mechanics Eng., April 19-21, MTC, Cairo, 2016
[2] Masahiro K., Fumio K. and Toru S. "Design Optimization Of Launch Vehicle Concept Using Cluster Hybrid Rocket Engine for Future Space Transportation" journal of fluid science and technology, vol. 11, No. 1, Paper No.15-00151, 2016
[3] Humble, R., Henry Gary N., Larson Wiley J., "Propulsion System Analysis and Design", United States Air Force Academy, 1995.
[4] Sutton G.: "Rocket Propulsion Elements", Sixth Edition, John Wiley, New York, 1992.
[5] Barrere M. et al., "Rocket Propulsion", Elsevier Publishing Company, 1960.
[6] Marxman C. A., Wooldridge C. E. and Muzzy R. J.: Fundamentals of hybrid boundary layer combustion, Heterogeneous combustion, progress in Astronauts and aeronautics, vol. 15, Academic press, New York, 1964.
[7] Wooldridge C. E. and Muzzy R. J. "Internal Ballistic Considerations in Hybrid Rocket Design", J. Spacecraft, Vol. 4, No. 2, Feb. 1967.
[8] David W. Netzer "Hybrid Rocket Internal Ballistics", Naval Postgraduate School, Monterey, January 1972.
[9] A. EL-S. Makled "Prediction of Hybrid Combustion Boundary Layer Parameters" 12th International Conference on Aerospace Sciences & Aviation Technology (ASAT-12), BAL-02, MTC, Cairo, May 29 – 31, 2007.
[10] Curt Selph "Computer Program for Calculation of Complex Chemical Equilibrium Composition", NASA SP-273, United States Air Force Academy, version, July 1994.

Ahmed El-S. Makled is a PhD academic doctor, worked in the aerospace engineering field, specialized in rocket propulsion, launch vehicle design and satellite launch services.

M. K. Al-Tamimiis a PhD student at the Military Technical College.